Shallow donors in magnetic fields in zinc-blende semiconductors. I. Theory

Witold Trzeciakowski
High Pressure Research Center (UNIPRESS), Polish Academy of Sciences, Sokolowska 29, PL-01-142 Warsaw, Poland

Michał Baj
Institute of Experimental Physics, Warsaw University, Hoza 69, PL-00-681 Warsaw, Poland

Serge Huant and Louis-Claude Brunel
Service National des Champs Intenses, Centre National de la Recherche Scientifique, Boîte Postale 166X, F-38042 Grenoble Cédex, France

(Received 3 September 1985)

In the weak-field regime (cyclotron energy $\lesssim$ effective Rydberg) the donor associated with the parabolic minimum of the conduction band may be treated as a hydrogen atom in a magnetic field. We review and compare the existing variational and adiabatic models pointing out those which are most useful for the analysis of magneto-optical data. In the high-field regime (cyclotron energy $\gg$ effective Rydberg) multiband ("nonparabolic") calculations are necessary. In this case we develop a new approach (analogue of the adiabatic method in the parabolic case) obtaining simple expressions for the energy levels, the wave functions, the selection rules, and the chemical shifts. In view of the recent high-pressure magneto-optical experiments we discuss the effect of pressure on all determined quantities. We also formulate the generalization of our multiband adiabatic approach.

I. INTRODUCTION

The increasing quantity and quality of magneto-optical data involving intradonor transitions in semiconductors[1-7] require more and more sophisticated and accurate theories to interpret the results. The problem of a donor (or an exciton) in a magnetic field has gained additional interest because of its similarity to the hydrogen atom in super strong magnetic fields, on white dwarfs[8] and pulsars.[9] However, even for a spherical and parabolic shape of the conduction-band edge (and this is the case for zinc-blende semiconductors at the Γ point of the Brillouin zone) there are important differences between the donor (or exciton) and the hydrogen atom.[10] The first consists in the presence of screening of the donor potential. The second arises for strong magnetic fields or large quantum numbers n when the Landau level energy $\hbar\omega_c(n+\frac{1}{2})$ becomes comparable to the gap width E_g. In such a case, the one-band, parabolic effective-mass approximation (EMA) is inadequate and should be replaced by a multiband ("nonparabolic") approach. If we express the magnetic field in dimensionless units $\gamma=\hbar\omega_c/(2\mathrm{Ry}^*)$ (Ry^* denotes the effective Rydberg) it turns out (see Sec. III) that the parabolic model of the donor works typically only up to $\gamma\sim 10$ for the ground state and fails at even lower γ for the excited states. For the hydrogen atom the "parabolic approach" also breaks down due to relativistic effects which, however, become important in a much higher region of γ ($\gamma\gtrsim 10^4$).

The high-field limit $\gamma\gtrsim 10$ can be achieved experimentally only for donors in narrow-gap semiconductors like InSb or $Hg_{1-x}Cd_xTe$ where 1 $\mathrm{Ry}^*\sim 1$ meV. Therefore most of the theoretical papers published as yet deal with the one-band, parabolic case. The energies were either obtained variationally[11-21] or by the so-called "adiabatic method" valid in the high-field limit.[22-26] In the last decade there has been a flood of papers in atomic physics and astrophysical journals devoted to the parabolic case (for a review see Ref. 27, more recent references may be found in Ref. 28). Various sophisticated numerical methods have been developed yielding very accurate results but at a high computational cost. Unfortunately many authors did not notice old solid-state papers, rediscovering some results. We review and compare various parabolic models in Sec. II. They are useful for the description of low-field donor states and they illustrate the quality of some approximations used in multiband models.

Previous multiband calculations (developed mainly for the interpretation of magneto-optical data in InSb) had some deficiencies which we wanted to avoid. The approach of Larsen[29] involves fairly complicated numerical calculations and yields the results for just a few donor states. The paper of Lin-Chung and Henvis[30] contains some errors which practically cancel the whole nonparabolic effect. Zawadzki and Wlasak[31] simplified the approach of Larsen and obtained general expressions for arbitrary donor states. They, however, neglected some important terms in the Hamiltonian so that their model overestimates the binding energies. Moreover, both Lin-Chung and Henvis and Zawadzki and Wlasak use fairly inaccurate trial functions. Therefore in Sec. III of this paper we develop a new multiband approach which yields simple expressions for arbitrary donor states. Nonparabolic effects become important in the high-field region, therefore we apply the trial functions accurate in that region. Our model may be regarded as a generalization of the adiabatic method to the multiband case. It is similar

to the approach introduced for the excitons by Rees[32] and by Altarelli and Lipari.[33] In Sec. III we determine the donor eigenstates in a Coulomb potential, the selection rules for the optical dipole transitions and the chemical shifts due to the localized portion of the impurity potential (in the first-order perturbation theory). We also present the generalization of our adiabatic approach so as to improve its accuracy in the low-γ region.

The transition energies and the chemical shifts are determined in magneto-optical experiments. Recently, such experiments were performed under high hydrostatic pressure,[6,7] therefore in Sec. IV we present our theoretical curves as a function of the magnetic field or of the pressure. Calculations are performed for donors in InSb and the results are compared with previous models. Their comparison with the experimental data is the subject of the following paper. The effect of pressure on the EMA Hamiltonian is discussed in Appendix A. Some useful matrix elements are given in Appendix B together with the simplified version of the parabolic calculation of Aldrich and Greene.[21] The exact expressions for the Landau states from the three-band model of Bowers and Yafet are shown in Appendix C.

II. PARABOLIC CASE

Within the one-band EMA the electron bound to a Coulombic donor in a uniform magnetic field $\mathbf{B}=(0,0,B)$ is described by the Hamiltonian[34]

$$\mathscr{H}=\frac{1}{2m^*}\left(\mathbf{p}-\frac{e}{c}\mathbf{A}\right)^2-\frac{e^2}{\epsilon_0 r}\ , \tag{1}$$

where $\mathbf{A}$ is the vector potential of the field, m^* and ϵ_0 are the effective mass and the dielectric constant, respectively. The simplified description of the screening, represented by ϵ_0 neglects two factors which may be important: (1) polaron effects (sometimes also described by the so-called dynamical screening[35]) substantial in polar crystals and (2) magnetic field effect on the screening (both interband and intraband) which will destroy the spherical symmetry of the potential. The first effect turns out to be negligible in InSb,[29] the second requires further investigations. In Eq. (1) the spin terms have been dropped as they only shift the energies by constant amounts, not influencing the transition energies. Choosing the symmetric gauge $\mathbf{A}=B/2(-y,x,0)$ and using the dimensionless atomic units [energy in $\mathrm{Ry}^*=m^*e^4/(2\hbar^2\epsilon_0^2)$, length in effective Bohr radii $a_B^*=\hbar^2\epsilon_0/(m^*e^2)$] we obtain

$$\mathscr{H}=\mathscr{H}_0-\frac{2}{(\rho^2+z^2)^{1/2}}\ , \tag{2a}$$

with

$$\mathscr{H}_0=-\nabla^2-i\gamma\frac{\partial}{\partial\varphi}+\frac{\gamma^2\rho^2}{4}\ , \tag{2b}$$

where $\gamma=\hbar\omega_c/(2\ \mathrm{Ry}^*)$ and the cylindrical coordinates ρ,φ,z were introduced. The fact that the Hamiltonian $\mathscr{H}$ (and thus also the energies and wave functions) depends only on one parameter γ facilitates the tabulation of the energies and can be used to obtain the values of some quantities from the experiment without even solving the Schrödinger equation[4,36] (this is no longer true in the multiband case). The form of $\mathscr{H}$ also implies that the magnetic field effect will be larger for more delocalized states while the Coulomb-field effect decreases with increasing ρ. The φ dependence separates in $\mathscr{H}$ so that the eigenstates will contain an $e^{iM\varphi}$ factor, M being the azimuthal quantum number. Another good quantum number is the parity $\pi=\pm1$ with respect to z. Because of the Coulomb term in (2) the Hamiltonian $\mathscr{H}$ is not separable and there are only approximate methods for determining its eigenstates. Different approaches have been developed in essentially two regions of γ: $\gamma\gg1$ hereafter denoted as the high-field region, and $\gamma\lesssim1$ further referred to as the low-field region. In the low-field region the eigenstates of $\mathscr{H}$ were usually constructed from the hydrogen like wave functions. In the high-field regime where the magnetic field terms dominate over the Coulomb potential (at least in the direction perpendicular to the field) the expansion in Landau states was more appropriate. The high-field region was important for astrophysicists ($\gamma\sim10^3$ on neutron stars) and for solid-state physicists ($\gamma\sim10^2$ in narrow-band-gap semiconductors). However, in the latter case the parabolic model fails at $\gamma\sim10$ (see Sec. III) and some effects of purely "nonparabolic origin" may arise even for $\gamma\sim1$ [e.g., spin doublets in GaAs (Ref. 37)]. Therefore the high-field case in semiconductors requires special treatment which will be developed in Sec. III.

A. Low-field region

For $\gamma\lesssim0.01$ the magnetic field terms in $\mathscr{H}$ can be treated as perturbations[27,28] (Zeeman effect). The levels are usually labeled as the zero-field states they originate from. In case of some excited states that are degenerate at $B=0$ one has to consider their appropriate combinations (e.g., $3d_0$ and $3s_0$). In the whole region $\gamma\lesssim1$ the best results for the eigenstates of $\mathscr{H}$ were obtained from the following expansion;

$$\psi_{M\pi}(r,\theta,\varphi)=\sum_l f_l(r)Y_{lM}(\theta,\varphi)\ , \tag{3}$$

where Y_{lM} are the spherical harmonics and the summation runs over even or odd values of l [the z parity of Y_{lM} equals $(-1)^{l-M}$]. Inserting (3) into the Schrödinger equation, multiplying by $Y_{lM}^*(\theta,\varphi)$ and integrating over the angles (see Refs. 38 and 28) we obtain a system of differential equations for $f_l(r)$ which may be solved numerically. The energies are tabulated in Ref. 28 for many low-lying states and for many values of $\beta=\gamma/2$. Very accurate energies for arbitrary fields may be obtained by interpolation. Several level crossings occur in the region $0.01<\gamma<1$. The wave functions obtained numerically were used to calculate the dipole matrix elements for various optical transitions and these were also tabulated in Ref. 28. Similar results have been obtained variationally by specifying the form of $f_l(r)$, usually as a linear combination of some given functions.[17,18] The variational problem then reduces to the eigenvalue problem for a finite order matrix. However, the above-mentioned methods although powerful, are fairly complicated nu-

TABLE I. The $(000)/1s$, $(0\bar{1}0)/2p_-$, and $(001)/2p_0$ binding energies versus γ obtained from various methods. The energies are in units of Ry*. The first row (data from Ref. 28) gives the most accurate estimates of the "true energies." Dashes indicate that the data were not available.

Method (1)	$\gamma=0$ (2)	$\gamma=1$ (3)	$\gamma=2$ (4)	$\gamma=5$ (5)	$\gamma=10$ (6)	$\gamma=20$ (7)	$\gamma=50$ (8)	$\gamma=100$ (9)	$\gamma=150$ (10)	$\gamma=500$ (11)
System of differential equations (Ref. 28)										
E_{000}	1.0000	1.6623	2.0444	2.7641	3.4956	4.4308	6.0439	7.5782	8.6367	12.532
$E_{0\bar{1}0}$	0.2500	0.9132	1.1992	1.7221	2.2508	2.9310	4.1199	5.2695	6.0710	9.076
E_{001}	0.2500	0.5200	0.5954	0.6961	0.7653	0.8268	0.8922	0.9272	0.9436	0.9753
Variational calculations of Larsen (Ref. 29)										
E_{000}	1.0000	1.6606	2.0412	2.750	3.4742	4.3915	5.956	7.457	8.477	12.229
$E_{0\bar{1}0}$	0.2500	0.9118	1.1973	1.717	2.2475	2.9270	4.108	5.261	6.062	9.059
E_{001}	0.2500	–	–	–	–	–	–	–	–	–
Modified variational calculations of AG[a] (see Appendix B)										
E_{000}	0.9922	1.6474	2.0324	2.7498	3.4854	4.4204	6.0234	7.564	8.616	12.490
$E_{0\bar{1}0}$	0.2468	0.9120	1.1982	1.7184	2.2496	2.9296	4.1116	5.266	6.064	9.055
E_{001}	0.2478	0.5191	0.5945	0.6940	0.7637	0.8247	0.8884	0.9234	0.9391	0.9691
Adiabatic										
E_{000}	0.00	1.3631	1.7995	2.5703	3.3370	4.2986	5.9320	7.4937	8.5565	12.4598
$E_{0\bar{1}0}$	0.00	0.8615	1.1543	1.6823	2.2184	2.9030	4.0908	5.2501	6.0500	9.0494
E_{001}	0.00	0.5069	0.5875	0.6915	0.7633	0.8257	0.8910	0.9271	0.9433	0.9750
Modified adiabatic (Refs. 24 and 25)										
E_{000}	–	1.66	2.05	2.76	3.48	4.42	6.05	7.69	–	–
$E_{0\bar{1}0}$	–	–	–	–	–	–	–	–	–	–
E_{001}	–	–	–	–	–	–	–	–	–	–
Variational calculations of YKA (Refs. 11 and 31)										
E_{000}	0.8488	1.5239	1.9081	2.6159	3.3313	4.2314	5.7552	7.2004	8.1764	11.7087
$E_{0\bar{1}0}$	0.2264	0.8919	1.1749	1.6868	2.2059	2.8662	4.0036	5.1030	5.8556	8.6368
E_{001}	0.2264	0.4919	0.5604	0.6463	0.7025	0.7482	0.7918	0.8135	0.8225	0.8385
Variational calculations of WB (Ref. 12)										
E_{000}	0.00	1.3462	1.7723	2.5200	3.2581	4.1763	5.7184	7.1738	8.1547	11.6973
$E_{0\bar{1}0}$	0.00	0.8564	1.1454	1.6640	2.1875	2.8517	3.9933	5.0952	5.8491	8.6332
E_{001}	0.00	0.4865	0.5579	0.6455	0.7022	0.7481	0.7918	0.8135	0.8225	0.8385

TABLE I. (*Continued*).

Method (1)	$\gamma=0$ (2)	$\gamma=1$ (3)	$\gamma=2$ (4)	$\gamma=5$ (5)	$\gamma=10$ (6)	$\gamma=20$ (7)	$\gamma=50$ (8)	$\gamma=100$ (9)	$\gamma=150$ (10)	$\gamma=500$ (11)
Variational calculations with the double Gaussian										
E_{000}	0.00	1.3622	1.7979	2.5670	3.3315	4.2895	5.9146	7.4658	8.5199	12.3811
$E_{0\bar{1}0}$	0.00	0.8614	1.1540	1.6816	2.2170	2.9004	4.0851	5.2400	6.0361	9.0152
E_{001}	0.00	0.5054	0.5852	0.6872	0.7570	0.8168	0.8780	0.9108	0.9252	0.9522
Variational calculations dG dL[b]										
E_{000}	0.00	1.4990	1.9268	2.6800	3.4310	4.3755	5.9842	7.5242	8.5724	12.4186
$E_{0\bar{1}0}$	0.00	0.8970	1.1868	1.7101	2.2423	2.9226	4.1034	5.2556	6.0503	9.0257
E_{001}	0.00	—	—	—	—	—	—	—	—	—
Correction factor for the dG[c]										
E_{000}	∞	1.2203	1.1371	1.0768	1.0493	1.0329	1.0219	1.0151	1.0137	1.0122
$E_{0\bar{1}0}$	∞	1.0601	1.0392	1.0241	1.0152	1.0106	1.0085	1.0056	1.0058	1.0067
E_{001}	∞	1.0289	1.0174	1.0130	1.0110	1.0122	1.0162	1.0180	1.0199	1.0243

[a] The ground state was calculated from the 9×9 matrix, both excited states from the 6×6 matrix.

[b] The trial function double Gaussian, double Landau given in Eq. (8).

[c] Ratio of the "exact" energies from Ref. 28 to those obtained with the double-Gaussian trial function.

merically. Therefore, if one is interested in obtaining the wave functions it is worthwhile to mention some variational calculations with simple forms of trial functions tending to hydrogen-atom states when $B\to 0$ (Refs. 29, 14, and 20). The best results were obtained in the approach of Larsen.[29] In Table I we have calculated some energies which for $\gamma \leq 10$ are only slightly worse than those from Ref. 28. Another approach that can be used to obtain fairly accurate energies and wave functions for arbitrary fields was introduced by Aldrich and Greene[21] and is discussed in the next section (and in Appendix B).

B. High-field region

We first introduce the eigenstates of $\mathscr{H}_0$ (Landau states) corresponding to the eigenvalues $\gamma(2n+1)+k^2$. In the adopted symmetric gauge they can be written in the form $\exp(ikz)F_{nM}(\rho,\varphi)$ where $M \leq n$ and

$$F_{nM}(\rho,\varphi)=\left[\frac{\gamma N!}{2\pi(N+|M|)!}\right]^{1/2} e^{iM\varphi}\sigma^{|M|/2}e^{-\sigma/2}\sum_{p=0}^{N}\binom{N+|M|}{N-p}\frac{(-\sigma)^p}{p!}, \tag{4}$$

with $N=n-\frac{1}{2}(M+|M|)$, $\sigma=\gamma\rho^2/2$. The eigenstates of the full Hamiltonian $\mathscr{H}$ can then be written as a combination of Landau states (they form a complete set) with arbitrary n and k (the Coulomb potential does not mix the states with different M values). Thus

$$\psi_{M\pi}(\rho,\varphi,z)=\sum_n g_n(z)F_{nM}(\rho,\varphi)\ , \tag{5a}$$

where

$$g_n(z)=\frac{1}{\sqrt{2\pi}}\int dk\,\alpha_n(k)e^{ikz}\ . \tag{5b}$$

Inserting (5a) into the Schrödinger equation, multiplying by $F^*_{nM}(\rho,\varphi)$ and integrating over ρ and φ we get a system of ordinary differential equations for $g_n(z)$:

$$-\frac{d^2}{dz^2}g_n(z)+\sum_{n'}V^M_{nn'}(z)g_{n'}(z)=[E-\gamma(2n+1)]g_n(z)\ , \tag{6a}$$

where

$$V^M_{nn'}(z)=-\int d\varphi\int d\rho\,\rho\frac{2}{(\rho^2+z^2)^{1/2}}F^*_{nM}F_{n'M}\ . \tag{6b}$$

Numerical solution of the system (6a) was obtained in Refs. 39 and 28 and again the extremely precise values of the energies for many states under the $n=0$ Landau level are tabulated in Ref. 28 as a function of $\beta=\gamma/2$. It turns out that with increasing γ the coupling between various Landau states decreases and for $\gamma\gg 1$ fairly accurate energies and wave functions can be obtained by retaining only one term in (5a), i.e.,

$$\psi_{M\pi}(\rho,\varphi,z)\cong g_n(z)F_{nM}(\rho,\varphi)$$
$$=\frac{1}{\sqrt{2\pi}}\int dk\,\alpha_n(k)e^{ikz}F_{nM}(\rho,\varphi)\ . \tag{7}$$

Consequently, the energies are obtained from a single equation (6a) with $V^M_{nn'}$ for $n'\neq n$ omitted. This is the so-called adiabatic approximation.[22,23,26] It consists in assuming that the donor states may be constructed solely from the nearest-lying Landau subband. The eigenstates are labeled by n, M, and β; last quantum number numerates various solutions of (6a) and equals the number of nodes of $g_n(z)$. The energies obtained from numerical solving of Eq. (6a) (with $V^M_{nn'}$ for $n'\neq n$ omitted) are shown in Table I. The adiabatic approximation, introduced in Refs. 22 and 23 can be also described as the assumption, that for strong fields the motion in the direction perpendicular to the field will be approximately the same as for the free Landau electron.

The modified adiabatic method introduced by Baldereschi and Bassani[24] and, independently, by Tanaka and Shinada[25] allows for the extension of its applicability down to $\gamma\approx 1$ (or even lower, for the excited states). The ground-state energies are shown in Table I. It can be seen that for $\gamma\gg 1$ this method slightly overestimates the binding energy because of neglecting some terms in the Hamiltonian (see Ref. 25).

There have been many variational calculations assuming the adiabaticlike form of the trial function: the pioneering works of Yafet *et al.*[11] (generalized in Ref. 31), Wallis and Bowlden,[12] and others.[13,15,16] In Table I we show the energies obtained from these simple but rather inaccurate approaches. These trial functions have also been applied in multiband calculations of Refs. 30 and 31. The errors introduced by poor trial functions can be comparable to the effects introduced by nonparabolicity (see Sec. III).

We also describe the method of Aldrich and Greene[21] somehow similar to the expansion in Landau states. It consists in constructing the wave function from Gaussians (in ρ and z variables) which yield simple analytical expressions for the matrix elements of $\mathscr{H}$. In Appendix B we show how to simplify the calculation of Aldrich and Greene if we are interested in the eigenstates of $\mathscr{H}$ which do not need to be orthogonalized (as is often the case for the observed donor states which differ either by the M value or by the parity). The original paper[21] was devoted to excitons where only the $M=0$ even-parity states are observable. Due to the simplification we obtained accurate energies (see Table I) by considering the matrices 9×9 (or 6×6) instead of 120×120. The results are good for any value of γ. For low and high fields one should take more Gaussians in the ρ and z direction, respectively. The trial functions of Yafet *et al.* and Wallis and Bowlden are the special cases of those of Aldrich and Greene. We also found that in the region $1<\gamma<500$ the adiabatic

method is practically equivalent to the variational calculation with the trial function $g_n(z)F_{nM}(\rho,\varphi)$, $g_n(z)$ being the combination of two Gaussians (see Appendix B). These double-Gaussian functions contain three variational parameters (in Table I we display the corresponding energies) and in view of their simplicity we have also used them in our multiband version of the adiabatic method (see Sec. III). The ratios of the "true energies" determined in Ref. 28 to the energies obtained with the double Gaussians are also shown in Table I (we shall call them correction factors for the double Gaussians).

Finally, in order to illustrate the superiority of the expansion (5) over the adiabatic assumption (7) (especially in the low γ region) we have calculated the binding energies variationally with the trial function being the combination of two Landau states:

$$\psi_{0M\beta}(\rho,\varphi,z)=\frac{f_0^\beta(z)F_{0M}(\rho,\varphi)+\alpha f_1^\beta(z)F_{1M}(\rho,\varphi)}{(1+\alpha^2)^{1/2}}, \tag{8}$$

where $f_0^\beta(z)$ and $f_1^\beta(z)$ were taken as double Gaussians of Appendix B. In (8) we have altogether seven variational parameters. The matrix elements of $\mathscr{H}$ can be easily expressed by those given in Appendix B and the resulting energies are shown in Table I.

Summarizing this section, the eigenstates of the parabolic Hamiltonian $\mathscr{H}$ [Eq. (2)] can be most precisely determined by numerical solution of the system of equations (6) in the high-field region or of the system resulting from the expansion (3) in the low-field region. Similar precision can be obtained in multiparameter variational calculations[17–19,21] although the restricted subspace of trial functions may cause some artifacts especially for the higher excited states. The energies of most of the observed states are tabulated in Ref. 28, together with the dipole matrix elements for optical transitions. Accurate and simple method for arbitrary magnetic field is the simplified version of Aldrich and Greene calculation, described in Appendix B. It can be used to determine the wave functions, which for $\gamma<100$ may also be obtained from the variational calculation of Larsen[29] or, for $\gamma>20$, from the adiabatic method. The adiabatic method for $1<\gamma<500$ is practically equivalent to the variational approach with a double-Gaussian trial function. Still, for donors in semiconductors it must be generalized to the multiband case (Sec. III). High precision of magneto-optical results require the similar precision of the theory (about 1%) therefore the simple trial functions of Refs. 11, 12, 15, and 20 are not sufficient.

It is interesting to note that there still exist controversies concerning the connection of the high-field (n,M,β) and the low-field (N,l,M) labeling of the eigenstates of (2) (see, e.g., Ref. 40). However, the best existing calculations confirm the noncrossing rule for the levels of the same M and parity.[28,39] This rule also implies that the (n,M,β) adiabatic levels with $M<n$ and $n\geq 1$ will merge into the continuum in the low-field region. The experimental evidence against the noncrossing rule[40] does not look convincing and the theoretical arguments are based on the modified adiabatic calculations[25,16] applied in the low-field region (where they are very inaccurate).

We also comment on the selection rules for the electric dipole transitions between the eigenstates of $\mathscr{H}$. As we mentioned, the oscillator strengths for many important transitions are tabulated in Ref. 28. For the accurate eigenfunctions they can be determined from the matrix elements of $(\mathbf{p}-e/c\,\mathbf{A})$ or $\mathbf{r}$ (see, e.g., Ref. 21). However, with the adiabatic functions which are correct for large r (where magnetic terms dominate the Coulomb terms) it is much better[28] to use the matrix elements of $\mathbf{r}$:

$$(\psi_{nM\beta}u_0\,|\,\mathscr{H}'\,|\,\psi_{n'M'\beta'}u_0)=\frac{ie\omega}{c}(\psi_{nM\beta}u_0\,|\,\mathbf{A}'\cdot\mathbf{r}\,|\,\psi_{n'M'\beta'}u_0), \tag{9}$$

where $\mathscr{H}'$ is the perturbation introduced by the radiation field with the vector potential $\mathbf{A}'(\mathrm{div}\,\mathbf{A}'=0)$, u_0 is the Bloch function at $\mathbf{k}=0$. Decomposing $\mathbf{A}'\cdot\mathbf{r}=A'_-r_+ +A'_+r_-+A'_zz$ with $r_\pm=(x\pm iy)/\sqrt{2}$, $A_\pm=(A_x\pm iA_y)/\sqrt{2}$ and using Eqs. (C7) from Appendix C we immediately obtain $\Delta\beta$ even, $\Delta n=0,\pm1$, $\Delta M=\pm1$ for $A'_\mp$ polarizations, and $\Delta\beta$ odd, $\Delta n=\Delta M=0$ for A'_z polarization. Using the momentum matrix elements [Eq. (C6)] in Eq. (9) we would not obtain the $\Delta n=0$ transitions for $A'_\mp$ which include the important $(000)\rightarrow(0\bar{1}0)$ line. Such a mistake was made, e.g., in Ref. 31. The selection rules for Δn do not hold in the low-field region, where many Landau states contribute to the wave function [see Eq. (5)]. In the high-field region for donors in semiconductors nonparabolic effects become important and the selection rules in that case will be considered in the next section.

III. NONPARABOLIC CASE

We start from a simple estimate of $\gamma=\hbar\omega_c/(2\ \mathrm{Ry}^*)$. Obviously $1\ \mathrm{Ry}^*=(m^*/m_0)(13.6\ \mathrm{eV})/\epsilon_0^2$. For two bands separated by the gap E_g we have $\hbar^2/m^*\sim P_0^2/E_g$ where P_0 is the standard momentum matrix element between the two bands. In most zinc-blende materials $m_0P_0^2/\hbar^2\sim10$ eV so that $\mathrm{Ry}^*\sim E_g/\epsilon_0^2$ and

$$\gamma\sim\frac{\hbar\omega_c}{2E_g}\epsilon_0^2. \tag{10}$$

Therefore in the region $\gamma\gg1$ we deal with $\hbar\omega_c$ comparable to the band gap. In such a case, the one-band EMA fails and we have to use a multiband approach.[10] This means that we choose a set of bands lying close to the conduction band (in zinc-blende structure one usually takes the Γ_6 conduction band, Γ_8 heavy- and light-hole bands, and the Γ_7 spin-orbit split-off valence band). The interaction between these bands is treated exactly while that with all other bands may be included in the second-order perturbation scheme.[34] In this way for the donor problem we obtain (in the appropriate basis of periodic functions from the Γ point)

$$\mathscr{H}=\mathscr{H}_0+V(\mathbf{r}), \tag{11}$$

where the "kinetic part" $\mathscr{H}_0$ already includes the magnetic field terms and is a finite order matrix operator (8×8 in the models of Bowers and Yafet[41] or Pidgeon and Brown[42]). The potential energy $V(\mathbf{r})$ is a diagonal matrix in the same representation. We assume that we know the eigenstates of $\mathscr{H}_0$ (conduction-band Landau states):

$$\mathscr{H}_0\psi^s_{nMk_z}=E^s_n(k_z)\psi^s_{nMk_z}\ , \tag{12}$$

which are multicomponent, slowly varying envelope functions. To obtain the total wave function the components of the envelope function should be multiplied by appropriate periodic amplitudes from the considered bands and summed up (see, e.g., Appendix C and Ref. 34). The index $s=\pm 1$ denotes two possible spin states. Generalizing the adiabatic method described in Sec. II B we assume that the eigenstate of $\mathscr{H}$ may be constructed solely from the Landau states of single (n,M,s) subband, i.e.,

$$\psi^s_{nM\beta}(\mathbf{r})=\int_{-\infty}^{+\infty}\alpha^\beta_k\psi^s_{nMk}(\mathbf{r})dk\ , \tag{13}$$

where k stands for k_z. This form of the donor envelope function guarantees its orthogonality to lower-lying eigenstates of $\mathscr{H}$. The Hamiltonian $\mathscr{H}_0$ possesses the eigenstates far below the conduction band, namely, the valence-band Landau states. These states are only slightly perturbed by the repulsive (for the holes) Coulomb potential and their mixing with the conduction-band Landau states can certainly be neglected. This "orthogonality problem" does not exist in the parabolic case.

The square modulus of the function (13) is

$$(\psi^s_{nM\beta}\,|\,\psi^s_{nM\beta})=\int|\alpha^\beta_k|^2(\psi^s_{nMk}\,|\,\psi^s_{nMk})dk\ . \tag{14}$$

The binding energy of the (n,M,β,s) donor state (expectation value of $\mathscr{H}$) becomes (with minus sign)

$$E^s_{nM\beta}=\left[\int dk[E^s_n(k)-E^s_n(0)]\,|\alpha^\beta_k|^2(\psi^s_{nMk}\,|\,\psi^s_{nMk})+\int dk\int dk'\,\alpha^{\beta*}_k\alpha^\beta_{k'}(\psi^s_{nMk}\,|\,V\,|\,\psi^s_{nMk'})\right]\Big/(\psi^s_{nM\beta}\,|\,\psi^s_{nM\beta})\ , \tag{15}$$

where we subtracted the subband-edge energy $E^s_n(0)$. Treating α^β_k as some trial function of k, we may choose it so as to minimize $E^s_{nM\beta}$. All we need are the eigenstates of $\mathscr{H}_0$. The double integral in Eq. (15) factorizes into independent integrals over k and k' so that the binding energy could be obtained numerically from the above equation. Please note that we avoid working with the complicated matrix $\mathscr{H}_0$ (compare, e.g., Refs. 29 and 31) immediately obtaining the scalar expression (15). In the following we shall specify $\mathscr{H}_0$ and we shall further simplify Eq. (15) in that particular case.

Fairly accurate description of the conduction band of zinc-blende materials and its magnetic field variation may be obtained from the model of Bowers and Yafet.[41] Three close lying Γ_6, Γ_7, and Γ_8 bands are taken into account, their interaction with all other bands is neglected. The energies of the Landau levels $E^\pm_n(k)$ and the corresponding wave functions $\psi^\pm_{nMk}$ are given in Appendix C. Equation (C2) allows one to calculate numerically the kinetic part in Eq. (15), for any assumed form of α^β_k. The potential energy in Eq. (15) becomes[43] [using Eqs. (C3) and (C4)]

$$\begin{aligned}(\psi^s_{nM\beta}\,|\,V\,|\,\psi^s_{nM\beta})=\int dz\Bigg[&|\phi^\beta(z)|^2V_{nM}(z)+3\gamma C\left(n+\frac{1-s}{2}\right)|f_{E_g}(z)|^2V_{n-s,M-s}(z)\\&+\gamma C\left(n+\frac{1+s}{2}\right)[\,|f_{E_g}(z)|^2+2\,|f_{E_g+\Delta}(z)|^2]V_{n+s,M+s}(z)\\&+C\left[2\left|\frac{df_{E_g}}{dz}\right|^2+\left|\frac{df_{E_g+\Delta}}{dz}\right|^2\right]V_{nM}(z)\Bigg]\ ,\end{aligned} \tag{16a}$$

where

$$\phi^\beta(z)=\frac{1}{\sqrt{2\pi}}\int dk\,\alpha^\beta_k e^{ikz}\ , \tag{16b}$$

$$f_E(z)=\frac{1}{\sqrt{2\pi}}\int dk\frac{\alpha^\beta_k e^{ikz}}{E+E^s_n(k)}\ , \tag{16c}$$

$$C=\frac{E_g(\Delta+E_g)}{2\Delta+3E_g}\ , \tag{16d}$$

and $V_{nM}(z)$ are given in Appendix B. Expression (16) may be further simplified if we note that the coefficients α^β_k of the expression (13) should be localized in the small-k region, consistently with the EMA (in atomic units we expect $k\sim 1$). In that region the variation of $E+E^s_n(k)$ in the denominator of Eq. (16c) can be ignored, so that

$$f_E(z)\cong\frac{\phi^\beta(z)}{E+E^s_n(0)}\ . \tag{17}$$

This means that we neglect terms of the order $k^2/[E_g+E^s_n(0)]\ll 1$. Consequently, two last terms in Eq. (16a) have to be rejected. The same approximation should be made in the kinetic energy part, i.e., the energy difference in Eq. (15) has to be determined from Eq. (C2) with the same accuracy. Also the norm of our eigenfunction [determined from Eq. (14) with the use of Eq. (C5)] simplifies if we neglect terms of the order of $k^2/[E_g+E^s_n(0)]$. In this way Eq. (15) becomes

$$E^s_{nM\beta}=-u^s_n\int_{-\infty}^{+\infty}\phi^{\beta*}\frac{d^2\phi^\beta}{dz^2}dz + \left[V_{nM\beta}+3\gamma C\frac{\left[n+\frac{1-s}{2}\right]}{(E_g+E^s_n)^2}V_{n-s,M-s,\beta}+\gamma C\left[n+\frac{1+s}{2}\right]\left[\frac{1}{(E_g+E^s_n)^2}+\frac{2}{(E_g+\Delta+E^s_n)^2}\right]V_{n+s,M+s,\beta}\right]\Big/M^s_n\,, \tag{18a}$$

with

$$u^s_n=\frac{C(3E^s_n+3E_g+2\Delta)}{(E^s_n+E_g)(E^s_n+E_g+\Delta)+E^s_n(2E^s_n+2E_g+\Delta)-3\gamma C(2n+1)}\,, \tag{18b}$$

and

$$M^s_n=1+\gamma C\left[\frac{(4n+2-s)}{(E_g+E^s_n)^2}+\frac{(2n+1+s)}{(E_g+\Delta+E^s_n)^2}\right], \tag{18c}$$

where $E^s_n=E^s_n(0)$ should be determined from Eq. (C2) and $V_{nM\beta}=\int|\phi^\beta(z)|^2V_{nM}(z)dz$. Here, instead of treating α^β_k as a trial function we use its Fourier transform $\phi^\beta(z)$. We have shown in Sec. II B that for $\gamma\gg1$ accurate results in the parabolic case may be obtained with the help of the double-Gaussian trial function, therefore we also use it here for $\phi^\beta(z)$. The formulas for the matrix elements appearing in Eq. (18a) for a few states observed in magnetooptical experiments are given in Appendix B; they can be written in a general (but cumbersome) form (see Ref. 31).

Equation (18a) differs from the corresponding equation (6a) obtained in the parabolic case (note that for $\gamma/E_g\to0$ they coincide). The potential energy is the weighted average of $V_{nM\beta}$, $V_{n+1,M+1,\beta}$, and $V_{n-1,M-1,\beta}$. This affects the binding energy in various ways. The second important modification introduced by nonparabolicity (erroneously neglected in Ref. 30) is the fraction in the kinetic energy part, representing simply the increasing effective mass at the bottom of the considered (n,s) Landau level. This fraction is always less than 1 (tends to one when $\gamma/E_g\to0$) so that the absolute value of the binding energy increases. For all considered states the second modification was more important than the first so that "nonparabolic energies" were larger than their parabolic counterparts. The effect of nonparabolicity increases with γ and is more pronounced for the excited states. It also increases with n due to the increasing effective mass. Numerical results will be discussed in Sec. IV.

Having determined the energy we can write down the formula for the wave function with the same accuracy, i.e., neglecting $k^2/(E_g+E^s_n)\ll1$. From Eqs. (13) and (14) with the help of Eqs. (C3), (C4), and (C5), we obtain the normalized donor eigenfunctions in the form[43]

$$\psi^+_{nM\beta}=\frac{1}{(M^+_n)^{1/2}}\left\{\phi^\beta F_{nM},\mp i\sqrt{3\gamma Cn}\frac{\phi^\beta F_{n-1,M-1}}{E_g+E^+_n},\mp i\sqrt{\gamma C(n+1)}\frac{\phi^\beta F_{n+1,M+1}}{E_g+E^+_n}\right.,$$
$$\left.\mp i\sqrt{2\gamma C(n+1)}\frac{\phi^\beta F_{n+1,M+1}}{E_g+\Delta+E^+_n},0,0,-i\sqrt{2C}\frac{\frac{d\phi^\beta}{dz}F_{nM}}{E_g+E^+_n},-i\sqrt{C}\frac{\frac{d\phi^\beta}{dz}F_{nM}}{E_g+\Delta+E^+_n}\right\}, \tag{19a}$$

$$\psi^-_{nM\beta}=\frac{1}{(M^-_n)^{1/2}}\left\{0,0,-i\sqrt{2C}\frac{\frac{d\phi^\beta}{dz}F_{nM}}{E_g+E^-_n},-i\sqrt{C}\frac{\frac{d\phi^\beta}{dz}F_{nM}}{E_g+\Delta+E^-_n},\phi^\beta F_{nM}\right.,$$
$$\left.\mp i\sqrt{3\gamma C(n+1)}\frac{\phi^\beta F_{n+1,M+1}}{E_g+E^-_n},\mp i\sqrt{\gamma Cn}\frac{\phi^\beta F_{n-1,M-1}}{E_g+E^-_n},\pm i\sqrt{2\gamma Cn}\frac{\phi^\beta F_{n-1,M-1}}{E_g+\Delta+E^-_n}\right\}, \tag{19b}$$

where the upper sign is for $M<0$, the middle for $M=0$, the lowest for $M>0$. The normalizing factor M^s_n is given in Eq. (18c). The components of the above vectors should be multiplied by the appropriate Bloch amplitudes $u_n(\mathbf{r})$, given in Appendix C. For arbitrary (n,M) and $\beta=0,1$ the functions $\psi^s_{nM\beta}$ are orthogonal. For $\beta=2,3,\ldots,$ they should be orthogonalized to all lower-lying states with the same (n,M) and the same parity. Neglecting the terms $k^2/(E_g+E^s_n)$ we obtain, that $\phi^\beta(z)$ with $\beta=2,3,\ldots,$ should be orthogonal to all $\phi^{\beta'}(z)$ with $\beta'<\beta$ of the same parity.

The above wave functions (together with periodic amplitudes) can be used to obtain the selection rules for electric dipole transitions between the $\psi^s_{nM\beta}$ states. Similarly to the parabolic case these selection rules should be determined from the matrix elements of $\mathbf{A}'\cdot\mathbf{r}$ and again it is

convenient to decompose $\mathbf{A}'\cdot\mathbf{r}=A'_-r_+ + A'_+r_- + A'_z r_z$. After some calculation we obtain, that for the spin conserving transitions $\Delta s=0$ we have the same selection rules as in the parabolic case: $\Delta\beta$ even, $\Delta M=\pm 1$, $\Delta n=0,\pm 1$ for the polarizations $A'_{\mp}$, $\Delta\beta$ odd, $\Delta M=\Delta n=0$ for the polarization A'_z. For fields such that $\gamma<10$ where our adiabatic approximation is not accurate, Δn may be arbitrary. This explains the observed intraimpurity transition with $\Delta n=2,3,\ldots$, reported in Ref. 44. However, with increasing field such transitions should vanish. Due to the fact that $\psi^s_{nM\beta}$ are not pure spin states, the spin-flip transitions ($\Delta s=\pm 2$) are possible. For $\Delta s=-2$, in the A'_+ polarization we get $\Delta M=0$, $\Delta n=0,1$, $\Delta\beta$ odd, in the A'_- polarization we have $\Delta M=2$, $\Delta n=1,2$, $\Delta\beta$ odd, in the A'_z polarization $\Delta M=\Delta n=1$, $\Delta\beta$ even. Unfortunately, in many cases the experiment does not confirm these simple rules,[7,45] indicating the presence of other perturbations, allowing for some "forbidden" transitions (e.g., the Coulomb fields of ionized impurities).

Formulas (19) can be used to determine important (and measurable) quantities, which are the chemical shifts of the donor states, originating from the localized portion of the impurity potential $V_{\rm loc}$. As long as the relative energy shifts due to $V_{\rm loc}$ are small, we can determine them from the first-order perturbation formula. We assume $V_{\rm loc}(\mathbf{r})$ to be tetrahedrally symmetric and localized in the region much smaller than the cyclotron radius or the Bohr radius. We can therefore expect that only the states nonvanishing at the impurity site ($\mathbf{r}=0$) will be affected by $V_{\rm loc}(\mathbf{r})$. In the parabolic adiabatic model only the states with $M=0$ and β pair can have nonzero chemical shifts. The form of our $\psi^{\pm}_{nM\beta}$ functions implies that we can also expect the chemical shifts for the states with $M=\pm 1$, β pair. For $M=0$ we obtain

$$\Delta E^s_{n0\beta}\cong(\psi^s_{n0\beta}\,|\,V_{\rm loc}\,|\,\psi^s_{n0\beta}) = \frac{1}{M^s_n}\frac{\gamma}{2\pi}\,|\,\phi^{\beta}(0)\,|^2(S\,|\,V_{\rm loc}\,|\,S)\,, \tag{20a}$$

and for $M=\pm 1$

$$\Delta E^s_{nM\beta}\cong(\psi^s_{nM\beta}\,|\,V_{\rm loc}\,|\,\psi^s_{nM\beta})=\frac{[n+\frac{1}{2}(1-M)]}{M^s_n}\gamma C\left[\frac{(2+Ms)}{(E_g+E^s_n)^2}+\frac{(1-Ms)}{(E_g+\Delta+E^s_n)^2}\right]|\,\phi^{\beta}(0)\,|^2\frac{\gamma}{2\pi}(X\,|\,V_{\rm loc}\,|\,X)\,, \tag{20b}$$

where S and X are periodic functions (see Appendix C) and the atomic units were used. When returning to ordinary units the above expressions should be multiplied by a_B^{*-3} (emerging from the volume element in the integrals). Here it may be noted that in previous nonparabolic models (Refs. 29 and 31) the wave functions had rapidly varying cusps at $\mathbf{r}=0$ [due to the presence of $V(\mathbf{r})$ in the denominators] so that $\psi(0)$ and, consequently, the chemical shifts were difficult to determine.

Before we proceed any further we comment on the accuracy of the approximations which we made. In the derivation of Eq. (18a) we have neglected the terms of the order $k^2/(E_g+E^s_n)$. In order to check this approximation we have calculated the energies E^+_{000} and E^+_{110} from the exact expressions (15), (16a), (14), (C2), and (C5), using a Fourier transform of the double Gaussian for α^0_k, i.e.,

$$\alpha^0_k=\frac{e^{-k^2/(\gamma\epsilon^2)}}{(\gamma\epsilon^2/2)^{1/2}}+\alpha\frac{e^{-k^2/(\gamma p\epsilon^2)}}{(\gamma p\epsilon^2/2)^{1/2}}\,. \tag{21}$$

The energies obtained from the exact expressions are shown in Table II together with the energies obtained from the approximate Eq. (18). In the calculations we used InSb parameters given in Sec. IV. The agreement is excellent (of the order of 0.1%) which proves that neglecting the terms $k^2/(E_g+E^s_n)$ was fully justified.

Another point which we investigated was the possible (due to nonparabolicity) coupling between $\psi^+_{nM\beta}$ and $\psi^-_{n'M'\beta'}$ states considered by some authors as important for the spin-flip transitions.[45] This coupling is possible only for $M+1=M'$ and it is proportional to Δ. Therefore the $(000+)$ ground state does not couple to any $(0,M',\beta'-)$ state but the $(0\bar{1}0+)$ state has a nonvanishing matrix element of $V(\mathbf{r})$ with $(001-)$. Still, we found that the influence of this coupling on binding energies was totally negligible (less than 0.01%) in agreement with the estimate of Larsen.[29]

It is important that in our treatment we approximate directly the binding energies which, for $\gamma\gg 1$, are only

TABLE II. The $(000+)$ and $(110+)$ binding energies in InSb determined from the exact expressions (14)–(16), (C2), and (C5) and those determined from Eq. (18) where the terms $k^2/(E_g+E^s_n)$ have been dropped.

	$\gamma=1$	$\gamma=10$	$\gamma=50$	$\gamma=100$	$\gamma=500$
E^+_{000}					
$E_{\rm exact}$	1.3622	3.3398	6.0418	7.8170	14.9281
$E_{\approx}$	1.3623	3.3406	6.0444	7.8211	14.9448
E^+_{110}					
$E_{\rm exact}$	0.8641	2.2929	4.6536	6.4260	13.9508
$E_{\approx}$	0.8641	2.2935	4.6583	6.4360	13.9890

small fractions of $E_n^{\pm}(0)$. If the binding energies are obtained by subtracting the approximate donor energy $E^{\pm}$ from $E_n^{\pm}(0)$, the relative error will increase. This was the case in Ref. 31 where the authors neglected the second and third power of the Coulomb potential and the commutators of $\mathbf{p}$ and V. It did not affect very much the total donor energy $E^{\pm}$ but changed significantly the binding energy $E_n^{\pm}(0)-E^{\pm}$. The YKA trial functions used in Ref. 31 are also far from being accurate (see Table I). Another nonparabolic calculation (Ref. 30), is based on even more simplified trial functions of Wallis and Bowlden (Table I) and contains an error in the kinetic energy part of $E_{nM\beta}^s$. Therefore up to now the only accurate nonparabolic approach was that of Larsen[29] where no important terms were neglected and the variational functions were very precise in the region $0\leq\gamma\leq 100$ (Table I). However, the model requires numerical two-dimensional integration and describes only the first few donor levels. We shall compare the results of Refs. 29 and 31 with our calculations in the following section.

In order to increase the accuracy of our approach in the low γ region we can proceed as in the parabolic case [see Eq. (5)], i.e., we may construct the donor wave function from many Landau states

$$\psi_{M\pi}^s=\sum_n\int dk\,\alpha_k^n\psi_{nMk}^s\ . \tag{22}$$

The spin mixing has been neglected here, as in the adiabatic model. Inserting (22) into the Schrödinger equation with $\mathscr{H}=\mathscr{H}_0+V$ we immediately obtain

$$\sum_n\int dk(E_n^s-E+u_n^sk^2+V)\alpha_k^n\psi_{nMk}^s=0\ . \tag{23}$$

Here we used the fact, that neglecting $k^2/(E_g+E_n^s)\ll 1$

$$E_n^s(k)\cong E_n^s+u_n^sk^2\ , \tag{24}$$

where u_n^s is the fraction defined in Eq. (18b). Projecting Eq. (23) on $\psi_{n'Mk'}^s$ we can use the explicit form of the Landau states [Eqs. (C3) and (C4)] and the exact values of their norms [Eq. (C5)]. Neglecting the terms $k^2/(E_g+E_n^s)$ and multiplying the resulting equation by $\int\exp(ik'z)dk'$ we obtain

$$\left[E_n^s-E-u_n^s\frac{d^2}{dz^2}\right]\phi_n(z)+\sum_{n'}\phi_{n'}(z)\left[V_{nn'}^M(z)+\frac{3\gamma C\left[\left[n+\frac{1-s}{2}\right]\left[n'+\frac{1-s}{2}\right]\right]^{1/2}}{(E_g+E_n^s)(E_g+E_{n'}^s)}V_{n-s,n'-s}^{M-s}(z)\right.$$
$$+\gamma C\left[\left[n+\frac{1+s}{2}\right]\left[n'+\frac{1+s}{2}\right]\right]^{1/2}$$
$$\left.\times\left[\frac{1}{(E_g+E_n^s)(E_g+E_{n'}^s)}+\frac{2}{(E_g+\Delta+E_n^s)(E_g+\Delta+E_{n'}^s)}\right]V_{n+s,n'+s}^{M+s}(z)\right]\Big/M_n^s=0\ , \tag{25}$$

where $V_{nn'}^M$ are defined in Eq. (6b), M_n^s is given in Eq. (18c). This is the multiband analogue of Eq. (6a). From the numerical point of view the modifications are small—the second derivative is multiplied by a constant u_n^s and the effective potential consists of three terms. Neglecting the coupling between different Landau states we arrive at the adiabatic Eq. (18a). The same sophisticated numerical methods that were used to solve the system of equations (6a) can be used to solve the system of equations (25).

IV. NUMERICAL RESULTS FOR InSb

We shall illustrate our results on the example of InSb, the best known narrow-gap material, available in excellent purity. The high-field limit $\gamma\gg 1$ can be easily achieved experimentally (at $B=1$ T $\gamma\cong 6.5$). For the three-band model of Bowers and Yafet we adopt the following parameters, taken from Ref. 46: $E_g(4.2\text{ K})=235.2$ meV, $\Delta=803$ meV, $P_0=-(i\hbar/m_0)(S\,|\,p_z\,|\,Z)=9.4\times10^{-8}$ eV cm. Under the hydrostatic pressure the gap E_g increases linearly with $dE_g/dP=140$ meV/GPa (Ref. 47) while Δ and P_0 may be assumed constant. The effective mass at the bottom of the conduction band can be written as

$$m^*=\frac{3\hbar^2}{2P_0^2}\frac{E_g(\Delta+E_g)}{(2\Delta+3E_g)}\ , \tag{26}$$

which yields $m^*(P=0)=0.01355m_0$. The dielectric constant for InSb $\epsilon_0(P=0)=16.8$ (Ref. 48) and its pressure dependence, calculated in our previous paper,[49] is given in Appendix A.

With the above set of parameters [$\text{Ry}^*(P=0)=0.653$ meV] we calculated from Eq. (18a) the binding energies of several donor states as a function of the magnetic field [Fig. 1(a) and 1(b)] and of the pressure at a fixed field [Fig. 1(c)]. For comparison we also show the binding energies from the parabolic model and those obtained from the nonparabolic models of Larsen[29] and Zawadzki-Wlasak.[31] In all models we used the same trial functions $\phi^{\beta}(z)F_{nM}(\rho,\varphi)$ where $\phi^{\beta}(z)$ are the double-Gaussians given in Appendix B (all necessary matrix elements are also listed[50] in Appendix B). We see that nonparabolicity increases all binding energies but this effect is overestimated

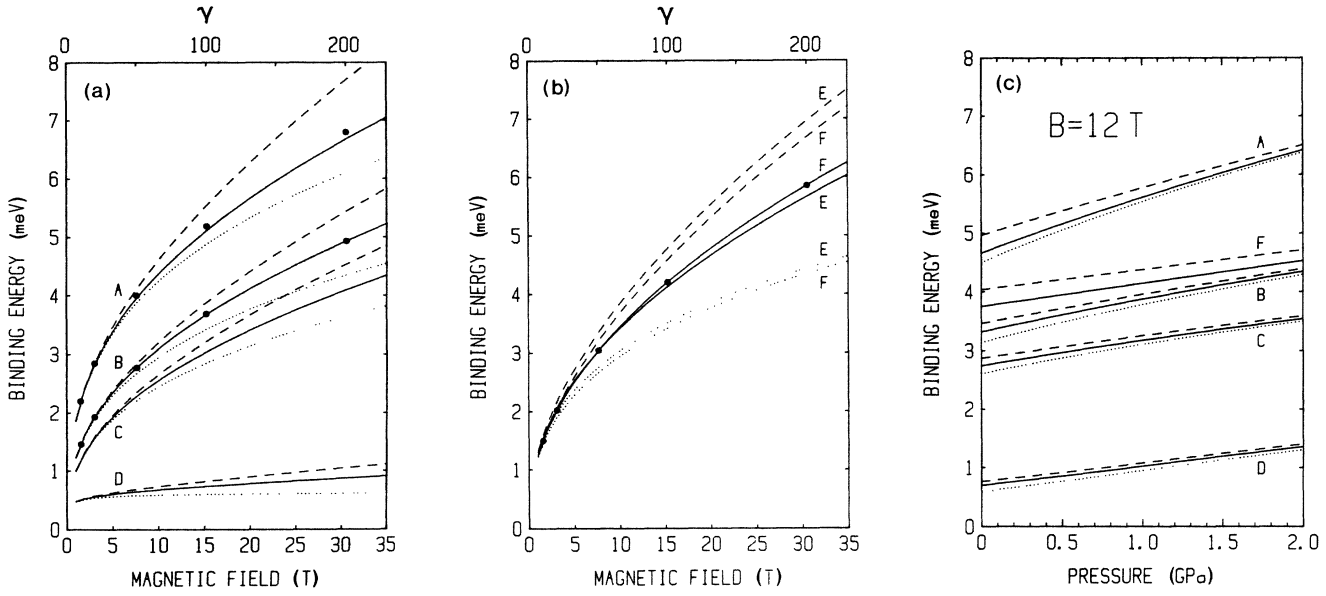

FIG. 1. Binding energies of several spin-up ($nM\beta$) donor states in InSb, shown as a function of magnetic field at $P=0$ [(a) and (b)] and as a function of pressure at the fixed $B=12$ T (c). Capital letters denote different levels: $A\equiv(000)/1s$, $B\equiv(0\bar{1}0)/2p_-$, $C\equiv(0\bar{2}0)/3d_{-2}$, $D\equiv(001)/2p_0$, $E\equiv(100)$, $F\equiv(110)/2p_+$ (there is no zero-field level for level E). Solid lines are calculated from our adiabatic three-band model, dotted lines represent the one-band (parabolic) calculation. Circles show the results of Larsen (Ref. 29) while the dashed lines were obtained from the model of Zawadzki and Wlasak (Ref. 31). In all of the models the same trial functions were used (double Gaussians).

in the calculation of Zawadzki and Wlasak for the reasons discussed in the preceding section. Up to $\gamma\cong 20$ the parabolic and nonparabolic models coincide. Our model predicts that the $(100+)$ and $(110+)$ levels cross so that at higher fields the $2p_+$ state becomes the lowest level associated with the $n=1$ Landau state. The results of Larsen coincide with ours, only if we use the same trial functions. However, from the numerical point of view our formula (18a) is extremely simple and more general as compared to the double integrals in Larsen's paper. If we compare Fig. 1 and the data from Table I we see the importance of the choice of proper trial functions. In some cases inaccurate trial functions may lead to larger errors than neglecting the whole nonparabolicity effect. The pressure dependence of the binding energies shown in Fig. 1(c) is rather weak and it should be obtained with the trial functions that have high accuracy in different regions of γ (high pressure increases m^* thus decreasing γ).

In Fig. 2 we show two quantities which vanish in the parabolic model; the difference between the binding energies $(E^+_{\bar{1}10}-E^+_{0\bar{1}0})$ and the differences $(E^-_{\bar{0}00}-E^+_{\bar{0}00})$, $(E^-_{0\bar{1}0}-E^+_{0\bar{1}0})$ (separation between the spin-flip energy and its hypothetical satellites[45]). Later we show that all of these energy differences would be almost unaffected by the central-cell potential. Again our results coincide with those of Larsen and differ substantially from those of Zawadzki and Wlasak.

In Fig. 3 we display the chemical shifts for the $(000\pm)$, $(0\bar{1}0\pm)$, and $(110+)$ states, calculated from Eq. (20). According to Ref. 51 we assumed $(S\,|\,V_{\rm loc}\,|\,S)=(X\,|\,V_{\rm loc}\,|\,X)=2.8\times10^{-21}$ eV cm^3. We see that the chemical shifts for the $|M|=1$ states are about an order of magnitude smaller than those for the $M=0$ states. The chemical shifts for $(000+)$ and $(000-)$ are almost identical, those for $(0\bar{1}0+)$ and $(0\bar{1}0-)$ differ significantly but due to their small values they should not influence the $(E^-_{0\bar{1}0}-E^+_{0\bar{1}0})$ energy difference. It is interesting to note that the $|M|=1$ chemical shifts decrease with pressure while those for $M=0$ increase.

V. SUMMARY AND CONCLUSIONS

In the field region corresponding to $\gamma<20$ the donor states can be usually well described by the one-band, parabolic models. In Sec. II we stressed the importance of the proper choice of the trial functions—for the first few states they can be obtained from the parabolic model of Larsen,[29] more general formulas follow from the simplified approach of Aldrich and Greene,[21] described in Appendix B. Very accurate values of the energies can be found by interpolating the tabulated data of Ref. 28.

In the high-field region nonparabolic (multiband) effects become important. We have shown how to generalize the adiabatic model to the multiband case. Adopting the simple description of the bands due to Bowers and Yafet[41] we obtained the variational adiabatic formulas (18a), (19), and (20) for the energies, wave functions, and the chemical shifts, respectively. We also gave the gen-

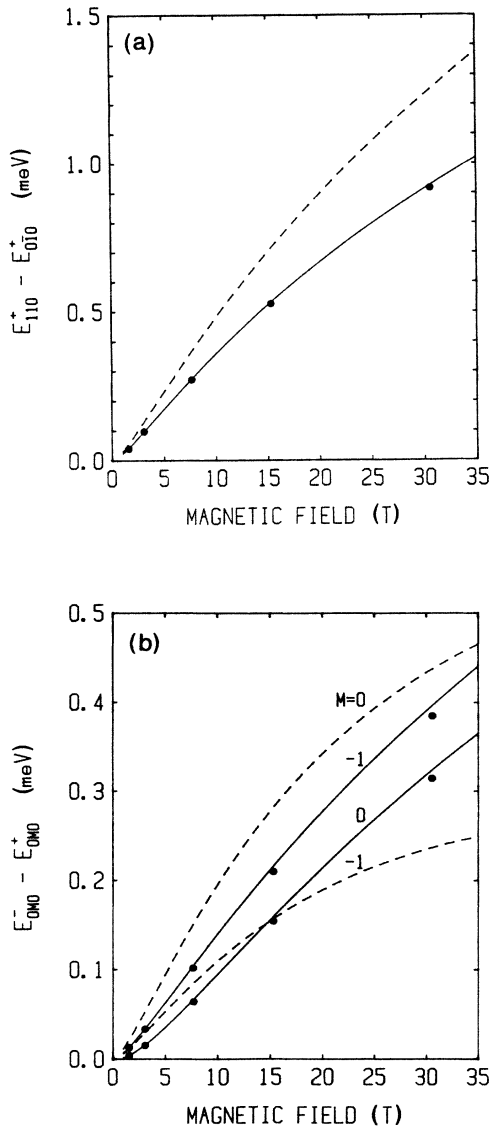

FIG. 2. (a) Energy difference $E^+_{110}-E^+_{0\bar{1}0}$ versus the magnetic field obtained from various models. It vanishes in the parabolic case. (b) Theoretical separation between the spin resonance $0^+\rightarrow 0^-$ and the hypothetical impurity spin resonances $(000+)\rightarrow(000-)$ and $(0\bar{1}0+)\rightarrow(0\bar{1}0-)$ obtained from various models. In the parabolic approach these resonances should coincide. Denotations as in Fig. 1.

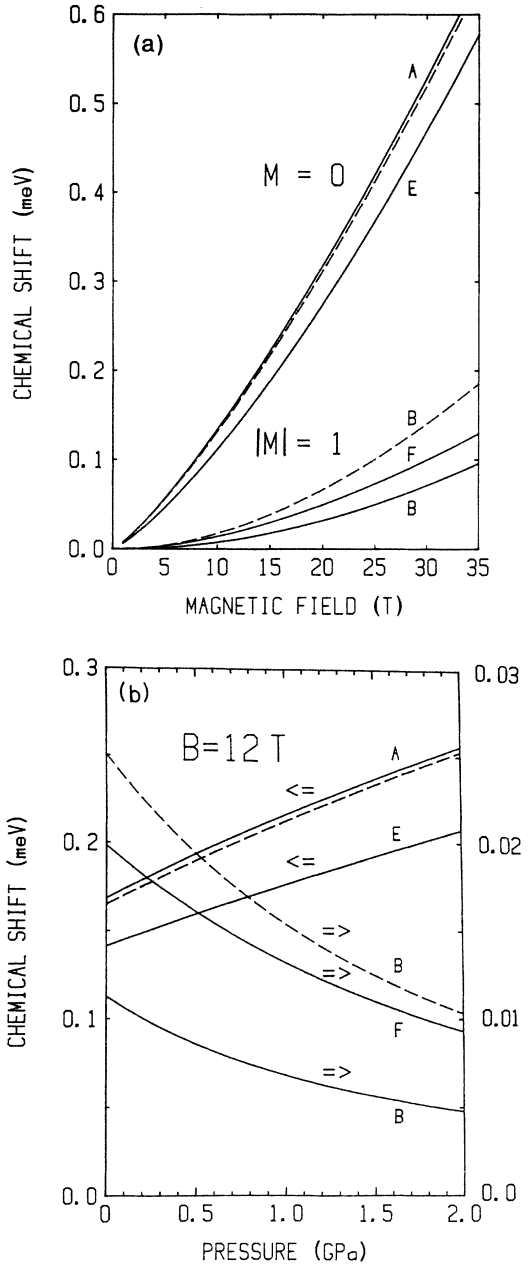

FIG. 3. Chemical shifts for the $(000\pm)$, $(0\bar{1}0\pm)$, $(100+)$, and $(110+)$ states calculated as a function of the magnetic field (a) and of the pressure (b). We adopted (Ref. 51) $(S\mid V_{\rm loc}\mid S)=(X\mid V_{\rm loc}\mid X)=2.8\times10^{-21}$ eV cm^3 independent of B and P. Solid lines are for the spin-up states ($s=+1$), dashed lines are for the spin-down states ($s=-1$). Levels are denoted as in Fig. 1.

eralized expansion into Landau states [Eq. (22)] and the corresponding system of equations (25) which can be solved numerically by the method of Ref. 28. Still, for $\gamma>20$ where the nonparabolic effects become important, the adiabatic approach is fairly accurate.

We can still point out two sources of inaccuracies, especially in the high-field limit: (1) The three-band model of Bowers and Yafet should be replaced by more sophisticated descriptions of the Landau states (e.g., from Ref. 42). Our approach can be applied to any multiband model although it would require more numerical work. (2) The description of the screening of the Coulomb potential represented by ϵ_0 is too simplified as it neglects the magnetic field effect and the polaron effects. We plan to investigate this in the near future.

ACKNOWLEDGMENTS

The authors are indebted to Dr. D. M. Larsen for sending us his unpublished results and to Professor W.

Zawadzki for valuable discussions. We are very much obliged to Mr. D. Wasik for his assistance in numerical calculations. Two of us (W.T. and M.B.) are grateful for the financial support of the Université Scientifique et Médicale de Grenoble during the initial stages of this work. The Service National des Champs Intenses is "Laboratoire associé á l'Université Scientifique et Médicale de Grenoble" and "Laboratoire propre No. 5021 du Centre National de la Recherche Scientifique."

APPENDIX A: EFFECT OF PRESSURE ON THE IMPURITY HAMILTONIAN

In the parabolic case the Hamiltonian (2) depends only on γ and the pressure enters through $m^*(P)$ and $\epsilon_0(P)$ dependences. With the increasing pressure the gap at $\mathbf{k}=0$ usually increases in zinc-blende materials which leads to the increase of m^* and the decrease of ϵ_0. Both of these factors cause the lowering of the γ value with pressure (e.g., in InSb at a fixed B the pressure of 1.7 GPa will decrease γ about 5 times).

In the three-band approach to the impurity problem, based on a Bowers-Yafet model of the band structure, the pressure may affect all parameters, i.e., E_g, Δ, P_0, and ϵ_0 (see Appendix C). The most important (and best known) is the $E_g(P)$ variation, Δ and P_0 are usually treated as constant. In InSb this seems to be a good approximation but in wider-gap materials the relative variation of $E_g(P)$ is weaker and might not be dominant. The effective mass at the bottom of the conduction band varies with pressure according to Eq. (26). It can also be determined experimentally in high-pressure cyclotron resonance measurements.[47]

The $\epsilon_0(P)$ dependence is difficult to measure in narrow-gap semiconductors. Therefore it has been calculated in Ref. 49 from the Ehrenreich-Cohen formula, with the energies and Bloch functions determined from the three-band model. For InSb the following formula has been obtained:

$$\epsilon_0(P)=16.8+\Delta\epsilon_0(P)-(0.026)(15.14P)-(0.035)(1.66P)\ , \tag{A1}$$

where P is in GPa and $\Delta\epsilon_0(P)$ is the "narrow-gap contribution" calculated in Ref. 49 and given in Table III. Expression (A1) was used in all our calculations for InSb.

TABLE III. Narrow gap contribution to $\epsilon_o(p)$ for InSb, calculated from the formulas given in Ref. 49.

P (GPa)	$-\Delta\epsilon_0(P)$	P (GPa)	$-\Delta\epsilon_0(P)$
0	0	0.8	0.386
0.1	0.059	0.9	0.423
0.2	0.114	1.0	0.459
0.3	0.166	1.2	0.526
0.4	0.215	1.4	0.588
0.5	0.261	1.6	0.645
0.6	0.305	1.8	0.698
0.7	0.346	2.0	0.747

APPENDIX B: MATRIX ELEMENTS OF THE HAMILTONIAN AND THE SIMPLIFIED METHOD OF ALDRICH AND GREENE

The matrix elements V_{nM} of the Coulomb potential between the F_{nM} Landau functions [see Eqs. (4) and (6b)] for $n=0$ can be written as

$$V_{0M}(z)=(-\gamma)^{|M|+1}\frac{z\sqrt{\pi}}{|M|!}\frac{d^{|M|}}{d\gamma^{|M|}}\left[\frac{\exp(\gamma z^2/2)}{(\gamma z^2/2)^{1/2}}Erfc\left[\frac{\gamma}{2}z^2\right]^{1/2}\right], \tag{B1}$$

where

$$Erfc(x)=1-Erf(x)=(2/\sqrt{\pi})\int_x^\infty \exp(-t^2)dt$$

and the atomic units were used. In many cases the formula

$$V_{nM}(z)=V_{n-M,-M}(z) \tag{B2}$$

may be found useful. When solving Eq. (6a) numerically it is better to use approximate expressions for the function $e^{x^2}Erfc(x)$ (e.g., the infinite fraction 7.1.14 from Ref. 52) and not the approximate expression for $Erfc(x)$ which, multiplied by e^{x^2}, become very inaccurate for large x.

We now describe the modified method of Aldrich and Greene[21] which we used to obtain accurate estimates of the energies in the parabolic case. The donor wave function is taken in the form

$$\psi^{Mq}(\rho,\varphi,z)=\sum_{k,l}C_{kl}^{Mq}\psi_{kl}^{Mq}(\rho,\varphi,z)\ , \tag{B3}$$

with

$$\psi_{kl}^{Mq}(\rho,\varphi,z)=e^{iM\varphi}z^q\rho^{|M|}e^{-\alpha_k\rho^2}e^{-\beta_l z^2}\ . \tag{B4}$$

Here $q=0$ or 1 determines the parity (with respect to z), α_k (or β_l) are chosen in geometric progression between $\alpha_{\min}$ and $\alpha_{\max}$ (or $\beta_{\min}$ and $\beta_{\max}$)

$$\alpha_k=\alpha_{\min}(\alpha_{\max}/\alpha_{\min})^{k/(N_\alpha-1)}\ ,\quad k=0,1,\ldots,N_\alpha-1 \tag{B5}$$

$$\beta_l=\beta_{\min}(\beta_{\max}/\beta_{\min})^{l/(N_\beta-1)}\ ,\quad l=0,1,\ldots,N_\beta-1\ . \tag{B6}$$

The coefficients C_{kl}^{Mq} are obtained from the eigenvalue problem for an $N_\alpha N_\beta\times N_\alpha N_\beta$ matrix. The functions ψ_{kl}^{Mq} are not orthogonal and their overlaps define the matrix $\underline{B}^{|M|q}$

$$B^{|M|\,q}_{kl,ij}=(\psi^{Mq}_{kl}\,|\,\psi^{Mq}_{ij})=\frac{\pi\,|M|\,!}{\alpha^{|M|+1}}\frac{(2q-1)!!}{(2\beta)^q}\left[\frac{\pi}{\beta}\right]^{1/2}, \tag{B7}$$

where we denote $\alpha=\alpha_k+\alpha_i$, $\beta=\beta_l+\beta_j$. The matrix elements of the "kinetic Hamiltonian" $\mathscr{H}_0$ are

$$(\psi^{Mq}_{kl}\,|\,\mathscr{H}_0\,|\,\psi^{Mq}_{ij})=[4\alpha_i(\,|M|+1)+\gamma M+2\beta_j(2q+1)]B^{|M|\,q}_{kl,ij}+\left[\frac{\gamma^2}{4}-4\alpha_i^2\right]B^{|M|+1,q}_{kl,ij}-4\beta_j^2B^{|M|,q+1}_{kl,ij}, \tag{B8}$$

while for the potential energy we obtain

$$\left[\psi^{Mq}_{kl}\left|\frac{-2}{r}\right|\psi^{Mq}_{ij}\right]=\frac{-4\pi(-1)^{|M|}}{(2q+1)}\frac{d^{|M|}}{d\alpha^{|M|}}\left[\alpha^{-q-1}F\left[q+\tfrac{1}{2},q+1,q+\tfrac{3}{2};1-\frac{\beta}{\alpha}\right]\right], \tag{B9}$$

where $F(a,b,c;x)$ is the hypergeometric function.[52] Using the property

$$\frac{d}{dx}F(a,b,c;x)=\frac{ab}{c}F(a+1,b+1,c+1;x), \tag{B10}$$

and the formula

$$F\left[\tfrac{1}{2},1,\tfrac{3}{2};1-\frac{\beta}{\alpha}\right]=\begin{cases}\dfrac{1}{2\left[1-\dfrac{\beta}{\alpha}\right]^{1/2}}\ln\dfrac{1+\left[1-\dfrac{\beta}{\alpha}\right]^{1/2}}{1-\left[1-\dfrac{\beta}{\alpha}\right]^{1/2}} & \text{for } \dfrac{\beta}{\alpha}\le 1,\\[2ex] \dfrac{1}{\left[\dfrac{\beta}{\alpha}-1\right]^{1/2}}\arctan\left[\dfrac{\beta}{\alpha}-1\right]^{1/2} & \text{for } \dfrac{\beta}{\alpha}\ge 1,\end{cases} \tag{B11}$$

we can obtain all necessary matrix elements of the potential in terms of elementary functions. The Schrödinger equation in the ψ^{Mq}_{kl} representation becomes

$$\underline{\mathscr{H}}^{Mq}\underline{C}^{Mq}=E\underline{B}^{|M|\,q}\underline{C}^{Mq}, \tag{B12}$$

so that the energies are given by the condition

$$\det[(\underline{B}^{|M|\,q})^{-1}\underline{\mathscr{H}}^{Mq}-E\mathbf{1}]=0. \tag{B13}$$

For each M and q we found the lowest root of (B13) and then we minimized it with respect to four parameters $\alpha_{\min}$, $\alpha_{\max}$, $\beta_{\min}$, and $\beta_{\max}$. The dimension of our basis (B4) is $N_\alpha N_\beta$ and very good values for all energies of interest in the range $0\le\gamma\le 500$ were already obtained for $N_\alpha=N_\beta=3$ (matrices 9×9). In their original approach[21] Aldrich and Greene were interested (for a given M and q) in several roots of Eq. (B13) and they minimized the trace of $(\underline{B}^{|M|\,q})^{-1}\underline{\mathscr{H}}^{Mq}$. They had to take $N_\alpha=10$, $N_\beta=12$ so that they were dealing with the matrices 120×120.

The adiabatic approximation can be introduced[53] into the method of Aldrich and Greene by fixing $N_\alpha=1$, $\alpha_0=\gamma/4$. The trial functions of Yafet *et al.* correspond to $N_\alpha=N_\beta=1$, those of Wallis and Bowlden are obtained for $N_\alpha=N_\beta=1$ and fixed $\alpha_0=\gamma/4$.

We shall now write down explicitly the matrix elements of the Hamiltonian between the adiabatic functions $F_{nM}(\rho,\varphi)\phi^\beta(z)$ with $\phi^\beta(z)$ taken as a normalized double Gaussian. For $\beta=0,1$

$$\phi^\beta(z)=\frac{(\gamma\epsilon^2)^{(2\beta+1)/4}}{(2\pi)^{1/4}}z^\beta\frac{e^{-1/4(\gamma\epsilon^2z^2)}+\alpha e^{-1/4(\gamma p\epsilon^2z^2)}}{M_\beta^{1/2}}, \tag{B14a}$$

with

$$M_\beta=1+\frac{\alpha^2}{p^{\beta+1/2}}+2\alpha\left[\frac{2}{p+1}\right]^{\beta+1/2}, \tag{B14b}$$

where ϵ,α, and p are variational parameters. The matrix elements of d^2/dz^2 and $V(r)$ between the $F_{nM}\phi^\beta$ functions can be obtained for $n=0$ from Eqs. (B8) and (B9). In our nonparabolic formula (18a) we need them also for $n\neq 0$. For $\beta=0,1$,

TABLE IV. Matrix elements of $V=-2/r$ between the single Gaussians of Wallis and Bowlden (Ref. 12). Here $A=(\gamma/2\pi)^{1/2}\epsilon$, $x=\epsilon^2$, $F_0=F(\frac{1}{2},1,\frac{3}{2};1-x)$ [see Eq. (B11)].

$G_{000}(\epsilon)=$	$-4AF_0$
$G_{0\bar{1}0}(\epsilon)=$	$-2A\left[\left[\dfrac{2-x}{1-x}\right]F_0-\dfrac{1}{1-x}\right]$
$G_{001}(\epsilon)=$	$\dfrac{-4A}{(1-x)}[-xF_0+1]$
$G_{100}(\epsilon)=$	$-\dfrac{A}{(1-x)^2}[(4-4x+3x^2)F_0-2-x]$
$G_{0\bar{2}0}(\epsilon)=$	$-\dfrac{A}{(1-x)^2}[(\frac{3}{2}x^2-4x+4)F_0-3+\frac{3}{2}x]$
$G_{0\bar{1}1}(\epsilon)=$	$-\dfrac{A}{(1-x)^2}[2x(x-4)F_0+4+2x]$
$G_{1\bar{1}0}(\epsilon)=$	$-\dfrac{A}{(1-x)^3}[(4-6x+\frac{15}{2}x^2-\frac{7}{4}x^3)F_0-3+x-\frac{7}{4}x^2]$
$G_{101}(\epsilon)=$	$-\dfrac{A}{(1-x)^3}[-3x(4+x^2)F_0+4+6x+5x^2]$

$$-\int_{-\infty}^{+\infty}\phi^{\beta}\frac{d^2\phi^{\beta}}{dz^2}dz=\frac{(2\beta+1)\gamma\epsilon^2}{4M_{\beta}}\left[1+\frac{\alpha^2}{p^{\beta-1/2}}+2\alpha p\left[\frac{2}{p+1}\right]^{\beta+3/2}\right], \tag{B15}$$

$$V_{nM\beta}=\int_{-\infty}^{+\infty}|\phi^{\beta}(z)|^2V_{nM}(z)dz=\frac{1}{M_{\beta}}\left\{G_{nM\beta}(\epsilon)+\frac{\alpha^2}{p^{\beta+1/2}}G_{nM\beta}(\epsilon\sqrt{p})+2\alpha\left[\frac{2}{p+1}\right]^{\beta+1/2}G_{nM\beta}\left[\epsilon\left[\frac{p+1}{2}\right]^{1/2}\right]\right\}, \tag{B16}$$

where $G_{nM\beta}(\epsilon)$ are the matrix elements of the potential between the "single Gaussians," i.e., the trial functions of Wallis and Bowlden[12] [given by Eq. (B14a) with $\alpha=0$]. General expressions for $G_{nM\beta}(\epsilon)$ are given in Ref. 31. Here we only list those that we needed in our nonparabolic formula (18a) for calculating $E^{\pm}_{\bar{0}00}$, $E^{\pm}_{\bar{0}10}$, $E^{\pm}_{\bar{0}20}$, $E^{\pm}_{\bar{0}01}$, $E^{\pm}_{\bar{0}11}$, $E^{\pm}_{\bar{1}00}$, and $E^{\pm}_{\bar{1}10}$ (see Table IV). Note that the property (B2) holds also for $V_{nM\beta}$, i.e., $V_{nM\beta}=V_{n-M,-M,\beta}$.

APPENDIX C: LANDAU STATES IN THE THREE-BAND MODEL OF BOWERS AND YAFET

In zinc-blende (or diamond) crystals the Bloch functions at $\mathbf{k}=\mathbf{0}$ from the Γ_6, Γ_7, and Γ_8 bands can be written in the form[41]

$$u_1=iS\uparrow\ ,\quad u_2=R_+\uparrow\ ,\quad u_3=\frac{1}{\sqrt{3}}R_-\uparrow+(\tfrac{2}{3})^{1/2}Z\downarrow\ ,$$
$$u_4=-(\tfrac{2}{3})^{1/2}R_-\uparrow+(\tfrac{1}{3})^{1/2}Z\downarrow\ ,\quad u_5=iS\downarrow\ ,\quad u_6=R_-\downarrow\ , \tag{C1}$$
$$u_7=-(\tfrac{1}{3})^{1/2}R_+\downarrow+(\tfrac{2}{3})^{1/2}Z\uparrow\ ,$$
$$u_8=(\tfrac{2}{3})^{1/2}R_+\downarrow+(\tfrac{1}{3})^{1/2}Z\uparrow\ ,$$

where $R_{\pm}=(X\pm iY)/\sqrt{2}$ and the arrows $\uparrow$ and $\downarrow$ mean spin-up and spin-down states, respectively. S and X, Y, Z are periodic functions which transform like atomic s and p functions under the operations of the tetrahedral group. The functions u_1 and u_5 correspond to the conduction Γ_6 band, u_2, u_3, u_6, and u_7 belong to the heavy- and light-hole Γ_8 band while u_4 and u_8 correspond to spin-orbit split-off Γ_7 band. If we neglect the effect of all other bands, the 8×8 Hamiltonian in u_n basis depends only on 3 parameters: band gap E_g, spin-orbit splitting Δ, and the momentum matrix element $P_0=-i\hbar/m_0(S\,|\,p_z\,|\,Z)$. The Schrödinger equation (in the presence of the uniform, static field $\mathbf{B}$) yields the flat heavy-hole band $E^{\pm}_{hh}\equiv-E_g$ and the following equation for the Landau states $E^{\pm}_n(k)$ associated with the conduction band, light-hole band and the spin-orbit split-off band

$$E(E+E_g)(E+E_g+\Delta)-C\{[\gamma(2n+1)+k^2](3E+3E_g+2\Delta)\mp\gamma\Delta\}=0\ , \tag{C2}$$

where C was defined in Eq. (16d). As usual, the atomic units were used. We shall be interested in the conduction-band states, given by the highest-lying (in energy) root of Eq. (C2). The eigenfunctions, corresponding to $E^{+}_n(k)$ have the following form

$$\psi^{+}_{nMk}=\frac{e^{ikz}}{\sqrt{2\pi}}\left[F_{nM},\pm\frac{i\sqrt{3\gamma Cn}}{E_g+E^{+}_n(k)}F_{n-1,M-1},\mp\frac{i\sqrt{\gamma C(n+1)}}{E_g+E^{+}_n(k)}F_{n+1,M+1}\ ,\right.$$
$$\left.\pm\frac{i\sqrt{2\gamma C(n+1)}}{E_g+\Delta+E^{+}_n(k)}F_{n+1,M+1},0,0,\frac{\sqrt{2C}k}{E_g+E^{+}_n(k)}F_{nM},\frac{\sqrt{C}k}{E_g+\Delta+E^{+}_n(k)}F_{nM}\right], \tag{C3}$$

and those corresponding to $E^{-}_n(k)$ are

$$\psi^{-}_{nMk}=\frac{e^{ikz}}{\sqrt{2\pi}}\left[0,0,\frac{\sqrt{2C}k}{E_g+E^{-}_n(k)}F_{nM},\frac{\sqrt{C}k}{E_g+\Delta+E^{-}_n(k)}F_{nM},F_{nM},\mp\frac{i\sqrt{3\gamma C(n+1)}}{E_g+E^{-}_n(k)}F_{n+1,M+1}\ ,\right.$$
$$\left.\mp\frac{i\sqrt{\gamma Cn}}{E_g+E^{-}_n(k)}F_{n-1,M-1},\pm\frac{i\sqrt{2\gamma Cn}}{E_g+\Delta+E^{-}_n(k)}F_{n-1,M-1}\right], \tag{C4}$$

where $M\le n$, F_{nM} are defined in Eq. (4), the upper signs are for $M<0$, the middle for $M=0$, and the lowest for $M>0$. The components of the vectors in Eqs. (C3) and (C4) should be multiplied by the corresponding u_n functions and summed up. The squared norms of the above Landau states are

$$(\psi^{\pm}_{nMk}\,|\,\psi^{\pm}_{nMk'})=\left\{1+C\left[\left[\frac{2}{[E_g+E^{\pm}_n(k)]^2}+\frac{1}{[E_g+\Delta+E^{\pm}_n(k)]^2}\right][\gamma(2n+1)+k^2]\right.\right.$$
$$\left.\left.\mp\gamma\left[\frac{1}{[E_g+E^{\pm}_n(k)]^2}-\frac{1}{[E_g+\Delta+E^{\pm}_n(k)]^2}\right]\right]\right\}\delta(k-k')\ . \tag{C5}$$

Our normalization is exact [provided that we determine exactly $E_n^{\pm}(k)$ from Eq. (C2)] contrary to previous papers[41] where it was only approximate. If we neglect the terms $k^2/[E_g+E_n^{\pm}(0)]$ the norms become k independent.

In the calculations involving "parabolic" Landau states $e^{ikz}F_{nM}$ and the "three-band" Landau states (C3) and (C4) we often made use of the following formulas (necessary also for determining the selection rules—see Sec. II)

$$P_+e^{ikz}F_{nM}=\mp i\hbar\sqrt{(n+1)\gamma}\,e^{ikz}F_{n+1,M+1}\ ,$$
$$P_-e^{ikz}F_{nM}=\pm i\hbar\sqrt{n\gamma}\,e^{ikz}F_{n-1,M-1}\ , \tag{C6}$$
$$P_ze^{ikz}F_{nM}=\hbar ke^{ikz}F_{nM}\ ,$$
$$r_+F_{nM}=\frac{1}{\sqrt{\gamma}}\begin{pmatrix}\mp\sqrt{n+1}F_{n+1,M+1}\pm\sqrt{n-M}F_{n,M+1}\\ +\end{pmatrix}\ ,$$
$$r_-F_{nM}=\frac{1}{\sqrt{\gamma}}\begin{pmatrix}\mp\sqrt{n}F_{n-1,M-1}\pm\sqrt{n-M+1}F_{n,M-1}\\ +\end{pmatrix}\ , \tag{C7}$$
$$r_zF_{nM}=zF_{nM}\ ,$$

where again the upper sign is for $M<0$, the middle for $M=0$, and the lower for $M>0$.

[1]R. Kaplan, Phys. Rev. **181**, 1154 (1969); Lecture Notes in Physics (Springer-Verlag, New York, 1980), Vol. 133, p. 138.

[2]C. J. Summers, R. Dingle, and D. E. Hill, Phys. Rev. B **1**, 1603 (1970).

[3]H. R. Fetterman, D. M. Larsen, G. E. Stillman, P. E. Tannenwald, and J. Waldman, Phys. Rev. Lett. **26**, 975 (1971).

[4]M. S. Skolnick, A. C. Carter, Y. Couder, and R. A. Stradling, J. Opt. Soc. Am. **67**, 947 (1977).

[5]L. E. Blagosklonskaya, E. M. Gershenzon, G. N. Goltsman, and A. I. Elantev, Bull. Acad. Sci. USSR, Phys. Ser. **42**, 1231 (1978).

[6]Z. Wasilewski, A. M. Davidson, R. A. Stradling, and S. Porowski, *Lecture Notes in Physics* (Springer-Verlag, New York, 1983), Vol. 177, p. 233.

[7]M. Baj, L. C. Brunel, S. Huant, W. Trzeciakowski, Z. Wasilewski, and R. A. Stradling, in *Proceedings of the 17th International Conference on the Physics of Semiconductors, San Francisco, 1984,* edited by J. D. Chadi and W. A. Harrison (Springer-Verlag, New York, 1985), p. 667.

[8]J. C. Kemp, J. P. Swedlund, J. D. Landstreet, and J. R. Angel, Astrophys. J. Lett. **161**, L77 (1970).

[9]M. Ruderman, Annu. Rev. Astron. Astrophys. **10**, 427 (1972); see also Garstang in Ref. 27 of this paper.

[10]Our description of the donor states is based on the effective-mass approximation which breaks down for very strong fields when the cyclotron radius becomes comparable to the lattice constant.

[11]Y. Yafet, R. W. Keyes, and E. N. Adams, J. Phys. Chem. Solids **1**, 137 (1956).

[12]R. F. Wallis and H. J. Bowlden, J. Phys. Chem. Solids **7**, 78 (1958).

[13]W. S. Boyle and R. F. Howard, J. Phys. Chem. Solids **19**, 181 (1961).

[14]E. Pokatilov and M. M. Rusanov, Fiz. Tverd. Tela (Leningrad) **10**, 3117 (1968) [Sov. Phys.—Solid State **10**, 2458 (1969)].

[15]R. Cohen, J. Lodenquai, and M. Ruderman, Phys. Rev. Lett. **25**, 467 (1970); the binding energies shown in this paper are erroneous.

[16]S. Narita and M. Miyao, Solid State Commun. **9**, 2161 (1971).

[17]J. Callaway, Phys. Lett. **40A**, 331 (1972).

[18]E. R. Smith, R. J. Henry, G. L. Surmelian, R. F. O'Connel, and A. K. Rajagopal, Phys. Rev. D **6**, 3700 (1972).

[19]H. C. Praddaude, Phys. Rev. A **6**, 1321 (1972).

[20]A. R. Rau and L. Spruch, Astrophys. J. **207**, 671 (1976).

[21]C. Aldrich and R. L. Greene, Phys. Status Solidi B **93**, 343 (1979).

[22]R. J. Elliott and R. Loudon, J. Phys. Chem. Solids **15**, 196 (1960).

[23]H. Hasegawa and R. E. Howard, J. Phys. Chem. Solids **21**, 179 (1961); H. Hasegawa, in *Physics of Solids in Intense Magnetic Fields,* edited by E. D. Haidemenakis (Plenum, New York, 1969), p. 246.

[24]A. Baldereschi and F. Bassani, Proceedings of the 10th International Conference on the Physics of Semiconductors, Boston, 1970 (unpublished), p. 191.

[25]K. Tanaka and M. Shinada, J. Phys. Soc. Jpn. **34**, 108 (1973).

[26]G. Wunner and H. Ruder, Astrophys. J. **242**, 828 (1980).

[27]R. H. Garstang, Rep. Prog. Phys. **40**, 105 (1977).

[28]W. Rösner, G. Wunner, H. Herold, and H. Ruder, J. Phys. B **17**, 29 (1984); H. Forster, W. Strupat, W. Rösner, G. Wunner, H. Ruder, and H. Herold, *ibid.* **17**, 1301 (1984).

[29]D. M. Larsen, J. Phys. Chem. Solids **29**, 271 (1968); the trial functions for some excited states are given in Phys. Rev. B **8**, 535 (1973); see also N. Lee, D. M. Larsen, and B. Lax, J. Phys. Chem. Solids **34**, 1059 (1973).

[30]P. J. Lin-Chung and B. W. Henvis, Phys. Rev. B **12**, 630 (1975).

[31]W. Zawadzki and J. Własak, in *Theoretical Aspects and New Developments in Magneto-Optics,* edited by J. T. Devreese (Plenum, New York, 1980), p. 347.

[32]G. J. Rees, J. Phys. C **5**, 549 (1972).

[33]M. Altarelli and N. O. Lipari, Phys. Rev. B **9**, 1733 (1974).

[34]For a rigorous derivation see, e.g., G. L. Bir and G. E. Pikus, *Symmetry and Strain Induced Effects in Semiconductors* (Wiley, New York, 1974).

[35]R. Enderlein, F. Bechstedt, and W. Hill, *Lecture Notes in Physics* (Springer-Verlag, New York, 1982), Vol. 152, p. 468.

[36]C. J. Armistead, F. Kuchar, S. P. Najda, S. Porowski, C. Sotomayor-Torres, R. A. Stradling, and Z. Wasilewski, *Proceedings of the 17th International Conference on the Physics of Semiconductors, San Francisco, 1984,* edited by J. D. Chadi and W. A. Harrison (Springer-Verlag, New York, 1985), p. 1047.

[37]D. M. Larsen, International Conference on Applications of High Magnetic Fields in Semiconductor Physics, Oxford, 1978, lecture notes (unpublished), p. 205.

[38]D. Cabib, E. Fabri, G. Fiorio, Il Nuovo Cimento **10B**, 185

(1972).
[39]J. Simola and J. Virtamo, J. Phys. B **11**, 3309 (1978).
[40]N. Kuroda, Y. Nishina, H. Hori, and M. Date, *Lecture Notes in Physics* (Springer-Verlag, New York, 1983), Vol. 177, p. 285.
[41]R. Bowers and Y. Yafet, Phys. Rev. **115**, 1165 (1959); W. Zawadzki, Lecture Notes in Physics (Springer-Verlag, New York, 1980), Vol. 133, p. 85.
[42]C. R. Pidgeon and R. N. Brown, Phys. Rev. **146**, 575 (1966).
[43]Throughout this section the atomic units from the bottom of the conduction band are used, i.e., the energy is measured in 1 $Ry^* = m^* e^4/(2\hbar^2\epsilon_0^2)$ and length in $a_B^* = \hbar^2\epsilon_0/(m^* e^2)$ where m^* is the effective mass at the band edge.
[44]S. Huant, L. C. Brunel, M. Baj, L. Dmowski, N. Coron, and G. Dambier, Solid State Commun. **54**, 131 (1985).
[45]F. Kuchar, R. Meisels, R. A. Stradling, and S. P. Najda, Solid State Commun. **52**, 487 (1984).
[46]M. W. Goodwin and D. G. Seiler, Phys. Rev. B **27**, 3451 (1983).
[47]S. Huant, L. Dmowski, M. Baj, and L. C. Brunel, Phys. Status Solidi B **125**, 215 (1984).
[48]J. R. Dixon and J. K. Furdyna, Solid State Commun. **35**, 195 (1980).
[49]W. Trzeciakowski and M. Baj, Solid State Commun. **52**, 669 (1984).
[50]We concentrate on the states with $\beta=0,1$. Those with $\beta\geq 2$ have not been observed in InSb probably because of the overlaps of the wave functions.
[51]I. Gorczyca, Phys. Status Solidi B **103**, 529 (1981).
[52]M. Abramowitz and J. A. Stegun, *Handbook of Mathematical Functions* (National Bureau of Standards, Washington, D.C., 1964).
[53]This works only for $n=0$ because the Landau functions $F_{nM}(\rho,\varphi)$ for $n>0$ may contain polynomials in ρ and cannot be expressed as a finite combination of Gaussian functions.